

³Jones, D. I. G., *Handbook of Viscoelastic Vibration Damping*, Wiley, New York, 2001, pp. 51–267.

⁴Eldred, L. B., Baker, W. P., and Palazotto, A. N., “Kelvin–Voigt vs Fractional Derivative Model as Constitutive Relations for Viscoelastic Material,” *AIAA Journal*, Vol. 33, No. 3, 1995, pp. 547–550.

⁵Sun, C. T., and Lu, Y. P., *Vibration Damping of Structural Elements*, Prentice–Hall, Upper Saddle River, NJ, 1995, pp. 210–238.

⁶Haug, E. J., Choi, K. K., and Komkov, V., *Design Sensitivity Analysis of Structural Systems*, Academic Press, London, 1986, pp. 49–70.

⁷Wang, S. M., and Choi, K. K., “Continuum Sizing Design Sensitivity Analysis of Eigenvectors Using Ritz Vectors,” *Journal of Aircraft*, Vol. 31, No. 2, 1993, pp. 457–459.

B. Balachandran
Associate Editor

Flowfield and Aerodynamic Performance of a Turbine Stator Cascade with Bowed Blades

Chunqing Tan*

Chinese Academy of Sciences, 100080 Beijing,
People's Republic of China

Atsumasa Yamamoto†

Japan Aerospace Exploration Agency,
Tokyo 182-8522, Japan

Haisheng Chen‡

Chinese Academy of Sciences, 100080 Beijing,
People's Republic of China

and

Shinpei Mizuki§

Hosei University, Tokyo 184-8584, Japan

Introduction

IN turbine stator cascades, the loss near the cascade endwalls contributes to the overall cascade loss significantly.¹ Therefore, it is very important to reduce this. The bowed blade (concept of which was published in the 1960s by Deich et al.²) has been considered by numerous researchers as the appropriate blade design to reduce the loss of turbine cascades. An experimental study with bowed stator blade cascade³ (here referred to as the Wang's cascade) was made and demonstrated that positive bowing could decrease the loss near the endwalls and made the spanwise distribution of the cascade outlet yaw angle uniform. The optimum bowed angle of about 20 deg was found to reduce the cascade loss by up to 40%. However, experiments performed by the present authors on another turbine stator cascade (Yamamoto's cascade) showed that the positive bowing neither reduced the cascade losses near the endwalls nor produced uniform distribution of the outlet yaw flow angle, and no optimum blade bowed angle was found.⁴ The different finding from

the two experiments is caused mainly by the different cascade setup (with and without the cascade tailgate), the Wang's tailgate extended 5 mm downstream from the blade trailing edge, which can lead to the measured cascade overall loss to include a jet loss at the cascade outlet. Thus, it is important to repeat the detailed experiments using the same Wang's cascade with more extended tailgate.

Experimental Method

The present experiment was conducted with a suction-type low-speed linear cascade wind tunnel at the Japan Aerospace Exploration Agency, Tokyo, Japan. The geometrical and aerodynamic parameters of the cascades presently tested are as follows: blade bowed angles $\varepsilon = 0, 10, 20$, and 30 deg (Fig. 1); blade height $h = 101.0$ mm; blade chord $C = 102.04$ mm; axial blade chord $C_{ax} = 69.0$ mm; blade pitch $T = 70.5$ mm; cascade outlet angle at the design $\alpha_{out,d} = 19$ deg (from the cascade pitchwise direction); outlet Mach number $M_{out} = 0.2$; Reynolds number $Re = 4.9 \times 10^5$; freestream turbulence intensity $T_u = 0.5\%$; inlet boundary-layer thickness $\delta_{99} = 24$ mm; and shape factor $\theta = 1.2$. The cascade outlet measurement plane was located at $0.45C_{ax}$ from the cascade trailing edge. The pitchwise measurement width was 129% of the cascade blade pitch. A five-hole pitot microprobe with head size of 1.5 mm was used to measure the cascade flowfields. The pressure measurement error was estimated at 0.15%. The energy loss coefficient is defined by

$$\xi = \frac{(P_s/P_t)^{(k-1)/k} - (P_s/P_{t,in})^{(k-1)/k}}{1 - (P_s/P_{t,in})^{(k-1)/k}} \quad (1)$$

where P_s , P_t , and $P_{t,in}$ represent local static pressure, local total pressure, and cascade inlet total pressure, respectively, and k ratio of specific heat. A detailed description of the experimental method and analysis method can be found in Ref. 4.

Results and Discussion

Figure 2 shows the energy loss coefficient at the outlet measurement plane. The loss distribution of the straight blade cascade

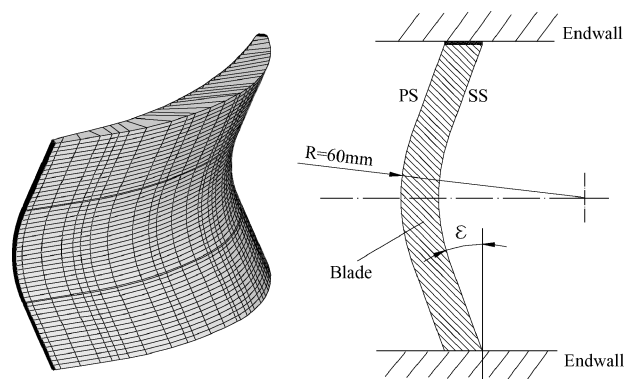
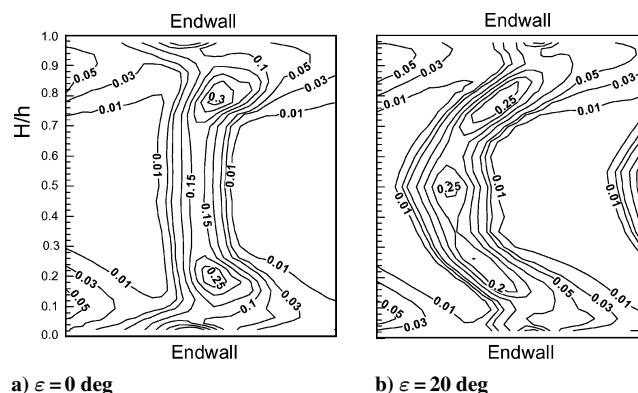


Fig. 1 Three-dimensional view and stacking lines of the bowed blades.



a) $\varepsilon = 0$ deg b) $\varepsilon = 20$ deg

Fig. 2 Distributions of the energy loss coefficient at the outlet measurement plane.

Received 7 April 2003; revision received 11 March 2004; accepted for publication 24 June 2004. Copyright © 2004 by the American Institute of Aeronautics and Astronautics, Inc. All rights reserved. Copies of this paper may be made for personal or internal use, on condition that the copier pay the \$10.00 per-copy fee to the Copyright Clearance Center, Inc., 222 Rosewood Drive, Danvers, MA 01923; include the code 0001-1452/04 \$10.00 in correspondence with the CCC.

*Professor, Institute of Engineering Thermophysics, P.O. Box 2706; tan@mail.etp.ac.cn. Member AIAA.

†Head, Turbomachinery Technology Development Team, Aeroengine Testing Technology Center, 7-44-1 Jindaiji Higashimachi, Chofu-shi; ayamamoto@chofu.jaxa.jp.

‡Ph.D. Student, Institute of Engineering Thermophysics, P.O. Box 2706; chen_hs@mail.etp.ac.cn.

§Professor, Department of Mechanical Engineering, 3-7-2 Kajino-cho, Koganei-shi; mizuki@fml.k.hosei.ac.jp.

($\varepsilon = 0$ deg) is similar to those of other conventional turbine stator cascades with low aspect ratio, such as in those used in Refs. 1 and 4. It is characterized by a pair of high loss cores at corner zones between each endwall and blade suction surface. When the blade bowed angle changes, loss coefficient contours change (as the center of the contours follow the blade bowed trailing-edge line) as shown in Fig. 2b. When the bowed angle increases, the loss around the blade midspan increases gradually as well, whereas the loss near both endwalls decreases as a result of the strengthened rolling up of the low energy fluids from the endwalls toward the midspan of the blade suction surface. This result is same as that presented in Ref. 4.

Figure 3a shows spanwise distribution of pitchwise mass-averaged energy loss ξ at the outlet measurement plane. When the bowed angle ε increases from 0 to 30 deg, the loss increases in the midspan region and decreases in the endwall regions. The overall mass-averaged energy loss ξ is within the range of 0.0535 ± 0.0015 for all of the cases (see Fig. 4). Therefore, the loss is not particularly affected by the bowed angles, which is different from the result given in Ref. 3 for the same Wang's blade profile (illustrated by the dashed lines in Fig. 3a). In Ref. 3, the loss of straight blade cascade near the endwalls was very high, which disagrees with the conventional loss distribution.^{1,5} When the blade is bowed from $\varepsilon = 0$ to 30 deg, the loss decreases in the endwall regions and increases slightly in the midspan region. Consequently, ξ of 20-deg bowed cascade is reduced by 40% from 0.098 (ξ of straight cascade) to 0.059 as shown in Fig. 4.

Figure 3b shows the spanwise distributions of the pitchwise mass-averaged yaw flow angles $\bar{\alpha}$ at the outlet measurement plane. When ε increases from 0 to 30 deg, $\bar{\alpha}$ near the endwalls increases, while $\bar{\alpha}$ around the midspan decreases. Thus, the distribution becomes more nonuniform as ε increases. The overall yaw flow angle $\bar{\alpha}$, for all

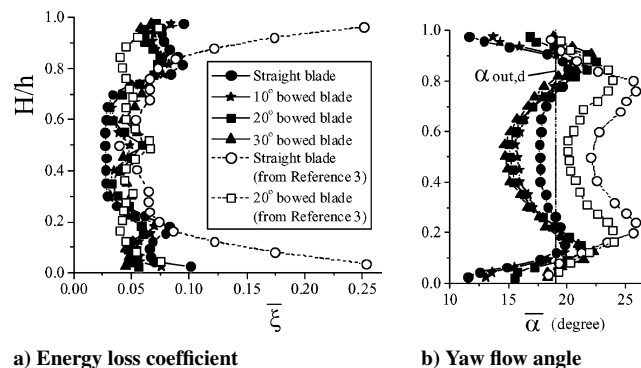


Fig. 3 Spanwise distributions of the pitchwise mass-averaged energy loss coefficient and yaw flow angle at the outlet measurement plane.

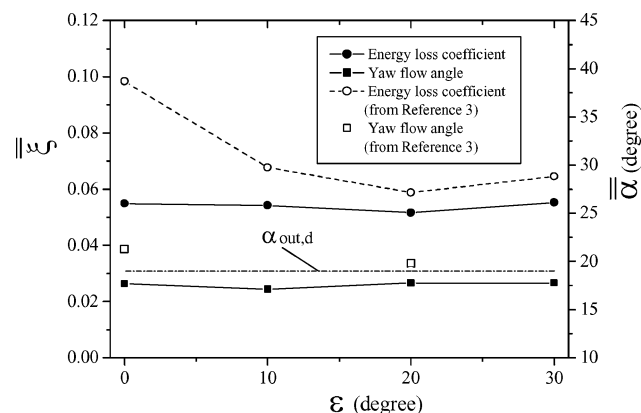


Fig. 4 Overall mass-averaged energy loss coefficient and yaw flow angle at the outlet measurement plane.

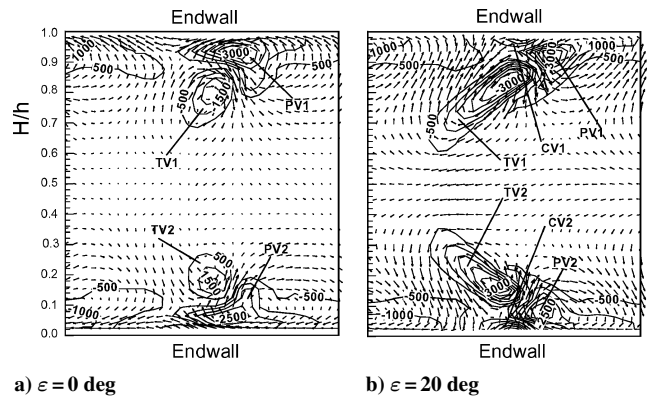


Fig. 5 Secondary flow vorticity contours and secondary flow vectors at the outlet measurement plane.

of the cases considered, are kept within 17.5 ± 0.4 deg as shown in Fig. 4 and not affected by ε , which is opposite to the result on $\bar{\alpha}$ given in Ref. 3 as indicated by the dashed lines in Fig. 3b.

Figure 5 shows secondary flow vorticity contours and secondary flow vectors at the outlet measurement plane. In Fig. 5, it is easy to find a pair of passage vortices (PVs), trailing vortices (TVs), and corner vortices (CVs). Vortices PV1 and PV2, TV1 and TV2, or CV1 and CV2 are approximately symmetrical to the cascade midspan, and the pairs' flow directions are opposite to each other. The horseshoe vortex formed at the blade pressure-side leading edge rolls up the large part of the lower energy fluids in the inlet endwall boundary layers to become a passage vortex (PV).⁵ When the bowed angle increases, the intensity, size, and location of PV1 and PV2 remain the same, and the losses near the both endwalls do not change significantly as evident in Fig. 3a. It is known that with the positive bowing the low-energy fluids on the cascade endwalls migrate more strongly to midspan region of the blade suction surface, which increases the loss around the blade midspan and decreases the loss near the endwalls (see Fig. 3a). Strength of the trailing vortices are indicated by TV1 and TV2. Stronger TVs lead to a larger turning angle of the flow around the midspan and decrease the yaw flow angles (see Fig. 3b).

Conclusions

For the turbine stator blade profile, the positive bowing neither reduces the cascade loss near the two endwalls nor makes the spanwise distribution of the outlet yaw flow angle uniform. No optimum blade bowed angle with minimum cascade overall loss could be determined. The present results using Wang's blade profile agree with the results of Ref. 4 using Yamamoto's blade profile, whereas they are different from those of Ref. 3 using the same Wang's blade profile. Influences of tailgate on the cascade performance should be considered carefully in the experiments.

References

- Yamamoto, A., "Production and Development of Secondary Flow and Losses Within Two Types of Straight Turbine Cascades, Part I: A Stator Case," *Journal of Turbomachinery*, Vol. 102, No. 2, 1987, pp. 186–193.
- Deich, M. E., Gubarev, A. B., Filipov, G. A., and Wang, Z., "A New Method of Profiling the Guide Vane Cascades of Turbine Stages with Small Diameter-Span Ratio," *Teplotoenergetika*, No. 8, 1962, pp. 42–46.
- Wang, Z., Han, W., Xu, W., and Zhao, G., "The Blade Curving Effects in a Turbine Stator Cascades with Low Aspect Ratio," Foreign Aerospace Science and Technology Center, Rept. AD-A261 063, Dayton, OH, Jan. 1993.
- Tan, C., Yamamoto, A., Mizuki, S., and Chen, H., "Influences of Blade Bowing on Flowfields of Turbine Stator Cascades," *AIAA Journal*, Vol. 41, No. 10, 2003, pp. 1967–1972.
- Severding, C. H., "Recent Progress in the Understanding of Basic Aspect of Secondary Flows in Turbine Blade Passages," *Journal of Engineering for Gas Turbine and Power*, Vol. 107, No. 2, 1985, pp. 248–257.

K. Fujii
Associate Editor